

# Effects of dust scattering in expanding spherical nebulae

M. Srinivasa Rao <sup>a,1</sup>, Sujan Sengupta <sup>a,2</sup>

<sup>a</sup>*Indian Institute of Astrophysics, Bangalore 560034, India*

---

## Abstract

The mean intensity of planetary nebulae with an expanding atmosphere is modeled by considering dusty and dust-free atmospheres. The bulk matter density is determined from the adopted velocity field through the equation of continuity. The gas is assumed to consist of hydrogen and helium and the gas-to-dust mass ratio is taken to be  $3 \times 10^{-4}$ . The Rayleigh phase function is employed for atomic scattering while the full Mie theory of scattering is incorporated for determining the dust scattering and absorption cross-section as well as the phase function for the angular distribution of photons after scattering. It is shown that in a dust free atmosphere, the mean intensity increases with the increase in the expansion velocity that makes the medium diluted. The mean intensity profile changes significantly when dust scattering is incorporated. The increase in forward scattering of photons by the dust particles yields into an increase in the mean intensity as compared to that without dust. The mean intensity increases as the particle size is increased. Thus it is shown that both the expansion of the medium and the presence of dust play important role in determining the mean intensity of a planetary nebulae.

*Key words:* planetary nebula – radiative transfer.

---

## 1 Introduction

There are several models of planetary nebulae which describe that the ionization structure and other physical characteristics (Hjellming 1966, Rubin 1968, Harrington 1968, 1969, Kirkpatrick 1970, 1972, Koppen 1979, 1980 ). They calculated the ionization structure by solving simultaneously, the equations of radiative transfer and ionization equilibrium for several elements such as

---

<sup>1</sup> E-mail: msrao@iiap.ernet.in

<sup>2</sup> E-mail: sujan@iiap.ernet.in

H, He, C, N, O, Ne, Mg, S, Ar etc. in different stages of ionization together with the energy equilibrium equation. The ionization equilibrium equation requires the use of the radiation in the form of mean intensity. Normally mean intensity obtained by the ‘on the spot approximation’ is utilized in evaluating the formation of hydrogen Ly  $\alpha$  line in dusty, expanding planetary nebulae. Infrared observations of planetary nebulae have established in the presence of dust (like graphite, amorphous carbon, silicate, and iron) in these objects and a comprehensive review work up to 1982 has been presented by Barlow (1983). Pottasch et al (1984), Iyengar (1986), Zijlstra et al (1989), Ratag et al (1990), Amnuel (1994). Pottasch et al. (1984) found infrared excesses in high dust temperature nebulae. They concluded the possibility of dust being mostly heated by the radiation of the central star on the long wave side since the nebulae are young. Ratag et al. (1990) suggested that the infrared excesses was due to the dust contents or heating by the interstellar radiation field. Amnuel (1994) favored the latter explanation. Peraiah and Wehrse (1978) found that the mean intensities of the radiation field are far different from those obtained from the ‘on the spot approximation’. The expansion in the nebulae would certainly modify the radiation field and this radiation field in turn changes the ionization structure in the nebulae. However, a complete and rigorous analysis by incorporating relevant theory for dust scattering in an expanding medium is not explored. In this paper we investigate the changes that are produced on the radiation field by the radially expanding gases and dust. For this purpose, we develop the solution of radiative transfer equation in the expanding nebulae. We assume both gas and dust with hydrogen and helium as the components of the gas. In section 2 we present the relevant radiative transfer equations that describes the radiation field under consideration. In section 3 we present the absorption cross section for atoms and dust. The adopted velocity law, the density distribution and the dust parameters are presented in section 4. The numerical method is described in section 5. The results are discussed in section 6 followed by our conclusion in section 7.

## 2 Radiative Transfer Equations

In a spherically symmetric, expanding, dusty planetary nebulae, the equations of radiative transfer can be written (Peraiah and Grant, 1973; henceafter PG73) as :

$$\begin{aligned} & \mu \frac{\partial U(r, \mu)}{\partial r} + \frac{1}{r} \frac{\partial}{\partial \mu} \left[ (1 - \mu^2) U(r, \mu) \right] + \sigma_g(r, \mu) U(r, \mu) + \sigma_d(r, \mu) U(r, \mu) \\ & = \sigma_g(r, \mu) \left[ \left( 1 - \omega_g(r) \right) B_g(r) + \frac{1}{2} \omega_g(r) \int_{-1}^{+1} p(r, \mu, \mu') U(r, \mu') d\mu' \right] \end{aligned}$$

$$+\sigma_d(r, \mu) \left[ \left(1 - \omega_d(r)\right) B_d(r) + \frac{1}{2} \omega_d(r) \int_{-1}^{+1} p(r, \mu, \mu') U(r, \mu') d\mu' \right] \quad (1)$$

for the outward-going rays, and

$$\begin{aligned} & -\mu \frac{\partial U(r, -\mu)}{\partial r} - \frac{1}{r} \frac{\partial}{\partial \mu} \left[ (1 - \mu^2) U(r, -\mu) \right] + \sigma_g(r, -\mu) U(r, -\mu) \\ & + \sigma_d(r, -\mu) U(r, -\mu) = \sigma_g(r, -\mu) \left[ \left(1 - \omega_g(r)\right) B_g(r) \right. \\ & \left. + \frac{1}{2} \omega_g(r) \int_{-1}^{+1} p(r, -\mu, \mu') U(r, \mu') d\mu' \right] + \sigma_d(r, -\mu) \\ & \left[ \left(1 - \omega_d(r)\right) B_d(r) + \frac{1}{2} \omega_d(r) \int_{-1}^{+1} p(r, -\mu, \mu') U(r, \mu') d\mu' \right] \end{aligned} \quad (2)$$

for the inward-going rays.

The quantity  $U(r, \mu)$  is given by,

$$U(r, \mu) = 4\pi r^2 I(r, \mu) \quad (3)$$

where  $I(r, \mu)$  is the specific intensity of the ray making an angle  $\cos^{-1} \mu$  with the radius vector at radial points  $r$ . We have restricted  $\mu = \cos \theta$  to lie in the interval  $(0,1)$ . Similarly,

$$B_{g,d}(r) = 4\pi r^2 b_{g,d}(r) \quad (4)$$

where the quantities  $b_{g,d}(r)$  are Planck functions for gas and dust respectively.  $\omega_g$  and  $\omega_d$  are the albedo's for single scattering for gas and dust. The quantities  $\sigma_g$  and  $\sigma_d$  are the absorption cross-sections for gas and dust.

### 3 Absorption Cross-section for Gas and Dust

For the absorption cross-section of hydrogen and helium we have (Hummer and Seaton 1964)

$$\begin{aligned} \sigma_H(\nu) &= 6.3 \times 10^{-18} \left( \frac{\nu_0}{\nu} \right)^3 \text{ cm}^2 & \text{if } \nu \geq \nu_0 \\ &= 0 & \text{if } \nu < \nu_0 \end{aligned} \quad (5)$$

for hydrogen and

$$\begin{aligned}\sigma_{He}(\nu) &= 7.35 \times 10^{-18} \exp \left[ -0.73 \left( \frac{\nu_0}{\nu} - 1.808 \right) \right] cm^2 \\ & \quad \text{if } \nu \geq 1.808 \nu_0 \\ & = 0 \quad \text{if } \nu < 1.808 \nu_0\end{aligned}\tag{6}$$

for helium. Here  $\nu_0$  is taken to be  $3.289 \times 10^{15}$  Hz which is hydrogen Lyman limit.

The calculations are being done in the rest frame and therefore, we have to modify the absorption cross section  $\sigma_H$  and  $\sigma_{He}$  in the rest frame by taking into account of the Doppler effect. The equation (5) and the (6) can be rewritten as (Landau and Lifshitz 1975)

$$\sigma_H^+(\nu) = 6.3 \times 10^{-18} \left[ \frac{\nu_0}{\nu} \left( 1 + \frac{v}{c} \mu \right) \right]^3 cm^2,\tag{7}$$

$$\sigma_H^-(\nu) = 6.3 \times 10^{-18} \left[ \frac{\nu_0}{\nu} \left( 1 - \frac{v}{c} \mu \right) \right]^3 cm^2\tag{8}$$

if  $\min \left[ \nu \left( 1 \pm \frac{v}{c} \mu \right) \right] \geq \nu_0$  and

$$\sigma_H^\pm(\nu) = 0\tag{9}$$

if  $\max \left[ \nu \left( 1 \pm \frac{v}{c} \mu \right) \right] < \nu_0$  for hydrogen. For helium,

$$\sigma_{He}^+(\nu) = 7.35 \times 10^{-18} \exp \left[ -0.73 \left\{ \left( \nu + \frac{v}{c} \mu \right) \frac{1}{\nu_0} - 1.808 \right\} \right]\tag{10}$$

and

$$\sigma_{He}^-(\nu) = 7.35 \times 10^{-18} \exp \left[ -0.73 \left\{ \left( \nu - \frac{v}{c} \mu \right) \frac{1}{\nu_0} - 1.808 \right\} \right]\tag{11}$$

if  $\min \left[ \nu \left( 1 \pm \frac{v}{c} \mu \right) \right] \geq 1.808 \nu_0$ ,

$$\sigma_{He}^{\pm}(\nu) = 0 \quad (12)$$

if  $\max\left[\nu\left(1 \pm \frac{v}{c}\mu\right)\right] < 1.808 \nu_0$ , where  $v$  is the radial velocity and  $c$  is the velocity of light. We have restricted our calculations up to a maximum frequency equal to  $\nu = 4 \times \nu_0$ . From equations (7), (8), (10) and (11) it is clear that

$$\begin{aligned} \sigma_g(r, \mu, \nu) &= \sigma_g^+(r, \nu) = \sigma_H^+(r, \nu) + \sigma_{He}^+(r, \nu) \\ \sigma_g(r, -\mu, \nu) &= \sigma_g^-(r, \nu) = \sigma_H^-(r, \nu) + \sigma_{He}^-(r, \nu) \end{aligned} \quad (13)$$

We have employed Rayleigh phase function that governs the angular distribution of photons after scattering with the atoms and is given by (Chandrasekhar 1960)

$$P(r, \mu, \mu') = \frac{3}{8}[3 - \mu^2 + (2\mu^2 - 1)\mu'^2] \quad (14)$$

For dust absorption and scattering we have employed the Mie theory of scattering (van de Hulst 1957). The extinction and scattering cross-section for dust scattering are given by

$$\sigma_d^{ext} = \frac{2\pi a^2}{x^2} \text{Real} [\sum_{n=1}^{\infty} (2n+1)(a_n + b_n)] \quad (15)$$

and

$$\sigma_d^{scat} = \frac{2\pi a^2}{x^2} \sum_{n=1}^{\infty} (2n+1)(|a_n|^2 + |b_n|^2) \quad (16)$$

where  $a$  is the radius of dust particles and  $x = 2\pi a/\lambda$ . The Mie coefficient  $a_n$  and  $b_n$  are in general complex function of the refractive index of the dust and of  $x$ . We have calculated the dust extinction and scattering cross section and hence the albedo  $\omega_d$  numerically for specific values of the dust size and refractive index. We have employed the full Mie phase function for the angular distribution of photons after scattering with dust.

#### 4 Model Parameters

We have adopted the usual power law for velocity profile which is given as

$$V(r) = V_0 + V_t \left(1 - \frac{R_{in}}{r}\right)^\gamma, \quad (17)$$

where  $V_0$  is the initial velocity at the inner radius  $R_{in} = 9.2568 \times 10^{16}$  cm, and  $V_t$  is the terminal velocity at  $R_{out} = 2.221632 \times 10^{17}$  cm taken from Osterbrock (1974, page 135). We fix the initial velocity  $V_0$  at  $0.1 \text{ kms}^{-1}$ . The terminal velocity  $V_t$  is considered to be 10, 20, 30, 50, 100 and 300  $\text{kms}^{-1}$ .

The distribution of total density comes from the equation of continuity and is written as

$$\rho(r) = \frac{\dot{M}}{4\pi r^2 V(r)} \quad (18)$$

where  $\dot{M}$  is the rate of mass loss. Since the particle number density in planetary nebulae ranges from 0.1 to 100  $\text{cm}^{-3}$ , we have set  $\dot{M} = 10^{-6} M_\odot \text{yr}^{-1}$ . The number density of He is taken to be 0.1 times that of H.

The dust-to-gas mass ratio for IC 418 and NGC 7662 are derived by Hoare (1990) to be  $6 \times 10^{-4}$  and  $3 \times 10^{-4}$  respectively. In our model we have taken dust-to-gas mass ratio as  $3 \times 10^{-4}$ . It is generally believed that dust in planetary nebula is carbon based one such as graphite. However, observation at infrared reveals the presence of silicates (Stasinska & Szczerba 1999; Pottasch 1987). Thus, we consider silicate type grains to demonstrate the effect of forward scattering. Now both the real and the imaginary refractive index for silicate grains are function of frequency and they depend on the grain composition. The real part of the refractive index for magnesium silicates such as Forsterite and Enstatite varies from 1.55 to 0.8 while the imaginary part varies from 0.85 to 0.3 (Scott & Duley 1996) in the frequency interval we have considered in the present work. For the sake of simplicity, in the present work we have taken an average value of the refractive indices for all the frequency points. The real part of the refractive index is taken to be 1.2 while the imaginary part is set at 0.5 for all frequency points. We have assumed same kind and size of spherical dust particles with radius 0.1 and 0.5 micron. It is worth mentioning that the Mie phase function reduces to that of Rayleigh when the ratio of the particle size to the wavelength is very small. Mie scattering is asymmetric in the sense that the forward scattering and the backward scattering are not the same while Rayleigh scattering is symmetric. The asymmetry parameter  $g = \langle \cos \theta \rangle$  is given by (Bohren & Huffman 1983)

$$\frac{1}{4} x^2 Q_{sca} \langle \cos \theta \rangle = \sum_n \frac{n(n+2)}{n+1} \text{Re}\{a_n a_{n+1}^* + b_n b_{n+1}^*\} + \sum_n \frac{2n+1}{n(n+1)} \text{Re}\{a_n b_n^*\}. \quad (19)$$

where  $Q_{sca}$  is the scattering efficiency and  $*$  denotes the complex conjugate. In fig 1, we present the asymmetry parameter for different frequency points with grain radii  $0.1 \mu m$  and  $0.5 \mu m$ . For Rayleigh scattering,  $g = 0$  because of symmetry. If the particle scatters more light toward the forward direction then  $g$  is positive while  $g$  is negative if the scattering is directed more toward the back direction. Although, the dust sizes considered is very small, the wavelength range that we are concerned is much shorter than the particle radius. As a consequence,  $g$  is positive in all frequency points considered in the present work. The numerical value of  $g$  very near to  $+1$  implies that the particles scatter light mostly in the forward direction. For a given frequency point the asymmetry increases as the particle size increases. On the other hand, for a given particle size, the asymmetry increases as the frequency increases. However, the asymmetry parameter depends on the refractive index as well. With the increase in the refractive index, the absorptivity of the particle increases. Fig 1 shows that  $g$  is almost constant with the particle radius  $0.5 \mu m$ . When the imaginary part of the refractive index is decreased from  $0.5$  to as small as  $0.02$ ,  $g$  increases with the increase in frequency and saturates at much higher value. The asymmetry parameter for different size of graphite grains is presented by Draine (1985). The Mie scattering and extinction cross-sections for astronomical silicates have been discussed in details by Draine & Lee (1984). At large value of  $x$ , the extinction efficiency  $Q_{ext}$  approaches to  $2.0$ . It is worth mentioning here that the dust opacity plays dominant role over the phase function in determining the emergent flux.

## 5 Numerical Method

The solution of radiative transfer in spherical symmetry (1) and (2) is developed by using discrete space theory of radiative transfer (PG73). In general the following steps are followed for obtaining the solution.

(i) We divide the medium into a number of "cells" whose thickness is less than or equal to the critical ( $\tau_{crit}$ ). The critical thickness is determined on the basis of physical characteristics of the medium.  $\tau_{crit}$  ensures the stability and uniqueness of the solution.

(ii) Now the integration of the transfer equation is performed on the "cell" which is two-dimensional radius - angle grid bounded by  $[r_n, r_{n+1}] \times [\mu_{j-\frac{1}{2}}, \mu_{j+\frac{1}{2}}]$  where  $\mu_{j+\frac{1}{2}} = \sum_{k=1}^j C_k$ ,  $j = 1, 2, \dots, J$ , where  $C_k$  are the weights of Gauss Legendre formula.

(iii) By using the interaction principle described in PG73, we obtain the reflection and transmission operators over the "cell".

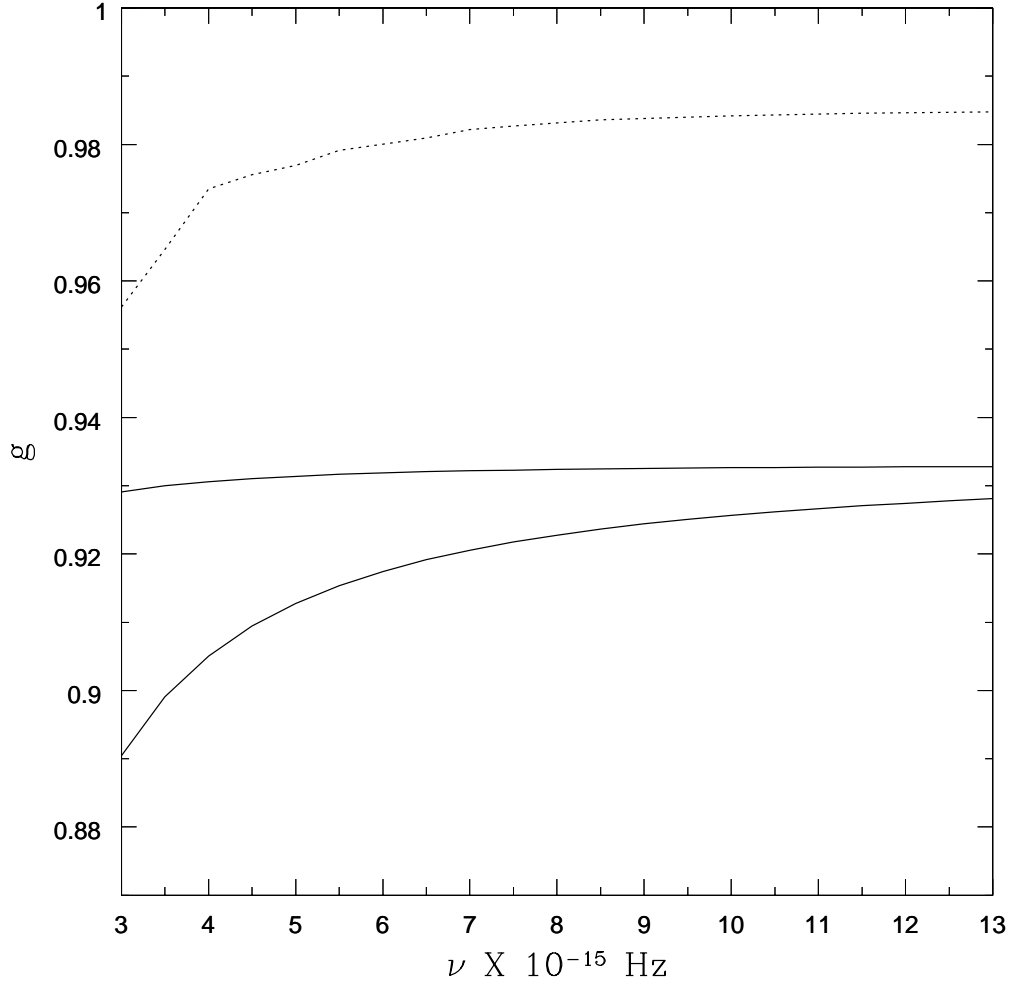


Fig. 1. The asymmetry parameter  $g$  with respect to the frequency. Top solid line represents the value of  $g$  for the particle radius  $0.5 \mu m$  while bottom solid line represents that for particle radius  $0.1 \mu m$ . The dashed line represents the value of  $g$  for particle radius  $0.5 \mu m$  but with imaginary refractive index 0.02

(iv) Finally we combine all the cells by the star algorithm described in PG73 and obtain the radiation field.

Now equation (1) and (2) can be rewritten upon  $\mu$  integration

$$\begin{aligned}
& M \frac{\partial U^+(r)}{\partial r} + \frac{1}{r} \left[ \Lambda^+ U^+(r) + \Lambda^- U^-(r) \right] + \sigma_g^+(r) U^+(r) \\
&= \sigma_g^+ \left[ 1 - \omega_g(r) \right] B_g^+(r) + \frac{1}{2} \omega_g \left[ P^{++}(r) C U^+(r) + P^{+-}(r) C U^-(r) \right] \\
&+ \frac{1}{2} \sigma_s \left[ P^{++}(r) C U^+(r) + P^{+-}(r) C U^-(r) \right] \tag{20}
\end{aligned}$$



and

$$\begin{aligned}
& -M \frac{\partial U^+(r)}{\partial r} - \frac{1}{r} \left[ \Lambda^+ U^+(r) + \Lambda^- U^+(r) \right] + \sigma_g^-(r) U^-(r) \\
& = \sigma_g^-(r) \left[ 1 - \omega_g(r) \right] B_g^-(r) + \frac{1}{2} \omega_g(r) \left[ P^{-+}(r) C U^+(r) + P^{--}(r) C U^-(r) \right] \\
& \quad + \frac{1}{2} \sigma_s \left[ P^{-+}(r) C U^+(r) + P^{--}(r) C U^-(r) \right] \tag{21}
\end{aligned}$$

$\omega_g$  and  $\omega_d$  are the albedo's for single scattering. Here,  $C$ ,  $M$ ,  $\sigma_g^-$  are the diagonal matrices of quadrature weights, angles and absorption cross-sections corresponding to the set of  $\mu$ 's.  $\Lambda^+$  and  $\Lambda^-$  are the curvature matrices defined in PG73, and

$$\mathbf{U}^\pm(\mathbf{r}) = \begin{pmatrix} U(r, \pm\mu_1) \\ U(r, \pm\mu_2) \\ U(r, \pm\mu_3) \\ \dots \\ U(r, \pm\mu_J) \end{pmatrix} \tag{22}$$

and

$$P^{++}(r) = P(r, +\mu, +\mu') \tag{23}$$

where  $0 < \mu_j < \mu_J \leq 1$ . We discretize equations (19) and (20) by integrating these equations from  $r_n$  to  $r_{n+1}$ . This gives us

$$\begin{aligned}
M \left[ U_{n+1}^+ - U_n^+ \right] + \tau_{g,n+\frac{1}{2}}^+ U_{n+\frac{1}{2}}^+ & = \tau_{g,n+\frac{1}{2}}^+ \left( 1 - \omega_g \right) B_{n+\frac{1}{2}}^+ \\
& \quad + \frac{1}{2} \left( \tau_d I + \tau_{g,n+\frac{1}{2}}^+ \omega_{g,n+\frac{1}{2}} \right) \left( P^{++} C U_{n+\frac{1}{2}}^+ + P^{+-} C U_{n+\frac{1}{2}}^- \right) \\
& \quad - \rho_c \left( \Lambda^+ U_{n+\frac{1}{2}}^+ + \Lambda^- U_{n+\frac{1}{2}}^- \right) \tag{24}
\end{aligned}$$

and

$$\begin{aligned}
M \left[ U_n^- - U_{n+1}^- \right] + \tau_{g,n+\frac{1}{2}}^- U_{n+\frac{1}{2}}^- & = \tau_{g,n+\frac{1}{2}}^- \left( 1 - \omega_g \right) B_{n+\frac{1}{2}}^- \\
& \quad + \frac{1}{2} \left( \tau_d I + \tau_{g,n+\frac{1}{2}}^- \omega_{g,n+\frac{1}{2}} \right) \left( P^{-+} C U_{n+\frac{1}{2}}^+ + P^{--} C U_{n+\frac{1}{2}}^- \right)
\end{aligned}$$

$$-\rho_c \left( \Lambda^- U_{n+\frac{1}{2}}^+ + \Lambda^+ U_{n+\frac{1}{2}}^- \right) \quad (25)$$

where the quantity with subscript  $n + \frac{1}{2}$  represents the average over the 'cell' bounded by the radii  $r_n$  and  $r_{n+1}$  (here, the 'cell' is defined as a shell with radial boundaries  $r_n$  and  $r_{n+1}$  and whose optical thickness is less than, or equal to the critical optical depth for which a stable and unique solution exists). Here,

$$\begin{aligned} \Delta r_{n+\frac{1}{2}} &= r_{n+1} - r_n \\ \tau_{g,n+\frac{1}{2}}^+ &= \sigma_{g,n+\frac{1}{2}}^+ \Delta r_{n+\frac{1}{2}} \end{aligned} \quad (26)$$

and  $\tau_d$  is parametrized. The quantity  $\rho_c$  is the curvature factor given by,

$$\rho_c = \frac{\Delta r_{n+\frac{1}{2}}}{r_{n+\frac{1}{2}}}, \quad (27)$$

where  $r_{n+\frac{1}{2}} = \frac{1}{2}(r_n + r_{n+1})$  is suitable mean radius and  $I$  is the identity matrix. The quantities  $U_{n+\frac{1}{2}}^\pm$  are approximated by those at the boundaries  $r_n$  and  $r_{n+1}$  by (see PG73)

$$U_{n+\frac{1}{2}}^\pm = \frac{1}{2} \left( U_n^\pm + U_{n+1}^\pm \right) \quad (28)$$

Substitution of equation (27) into equation (23) and (24) would give us the system of equations in the form of interaction principle and the result is written as

$$\begin{aligned} \begin{pmatrix} X_{11} & X_{12} \\ X_{21} & X_{22} \end{pmatrix} \begin{pmatrix} U_{n+1}^+ \\ U_n^- \end{pmatrix} &= \begin{pmatrix} Y_{11} & Y_{12} \\ Y_{21} & Y_{22} \end{pmatrix} \begin{pmatrix} U_{n+1}^+ \\ U_n^- \end{pmatrix} \\ &+ (1 - \omega_g) \begin{pmatrix} \tau_g^+ & B^+ \\ \tau_g^- & B^- \end{pmatrix} \end{aligned} \quad (29)$$

where

$$\begin{aligned} X_{11} &= M + \frac{1}{2}\tau_g^+ - \frac{1}{2}T^+P^{++}C + \frac{1}{2}\rho_c\Lambda^+ \\ X_{12} &= -\frac{1}{2}T^+P^{++}C + \frac{1}{2}\rho_c\Lambda^- \end{aligned}$$

$$\begin{aligned}
X21 &= -\frac{1}{2}T^-P^{-+}C + \frac{1}{2}\rho_c\Lambda^- \\
X22 &= M - \frac{1}{2}\tau_g^+ - \frac{1}{2}T^-P^{--}C - \frac{1}{2}\rho_c\Lambda^+ \\
Y11 &= M - \frac{1}{2}\tau_g^+ + \frac{1}{2}T^+P^{++}C - \frac{1}{2}\rho_c\Lambda^+ \\
Y12 &= \frac{1}{2}T^+P^{+-}C - \frac{1}{2}\rho_c\Lambda^- \\
Y21 &= \frac{1}{2}T^-P^{-+}C + \frac{1}{2}\rho_c\Lambda^- \\
Y22 &= M - \frac{1}{2}\tau_g^- + \frac{1}{2}T^-P^{--}C + \frac{1}{2}\rho_c\Lambda^+
\end{aligned}$$

where

$$T^\pm = \frac{1}{2}[\tau_d I + \tau_g^\pm \omega] \quad (30)$$

Comparing this with the interaction principle,

$$\begin{pmatrix} U_{n+1}^+ \\ U_n^- \end{pmatrix} = \begin{pmatrix} t(n+1, n) & r(n, n+1) \\ r(n+1, n) & t(n, n+1) \end{pmatrix} \times \begin{pmatrix} U_n^+ \\ U_{n+1}^- \end{pmatrix} + \begin{pmatrix} \Sigma_{n+\frac{1}{2}}^+ \\ \Sigma_{n+\frac{1}{2}}^- \end{pmatrix} \quad (31)$$

where  $t$ 's and  $r$ 's are the transmission and reflection operators. The quantities  $\Sigma_{n+\frac{1}{2}}^\pm$  are the source vectors. By comparing equations (28) and (30) one obtains the reflection and transmission operators. These are given in the appendix.

## 6 Results and Discussion

As the purpose of this paper is to show the qualitative changes introduced by curvature and expansion. We have chosen Harrington's (1969) model of NGC 7662 given in Osterbrock (1974, page 135). Few discrete points in the frequency grid are considered starting  $3.289 \times 10^{15}$  Hz to about four times this frequency. We have divided this frequency interval into 20 points equally distributed along the grid. The mean intensity is calculated by using the relation

$$J_\nu = \frac{1}{2} \int_{-1}^{+1} I(\mu) d\mu. \quad (32)$$

The results are presented in figure 2-5. Figure 2 shows the mean intensity without the effect of dust scattering and absorption. The mean intensity increases

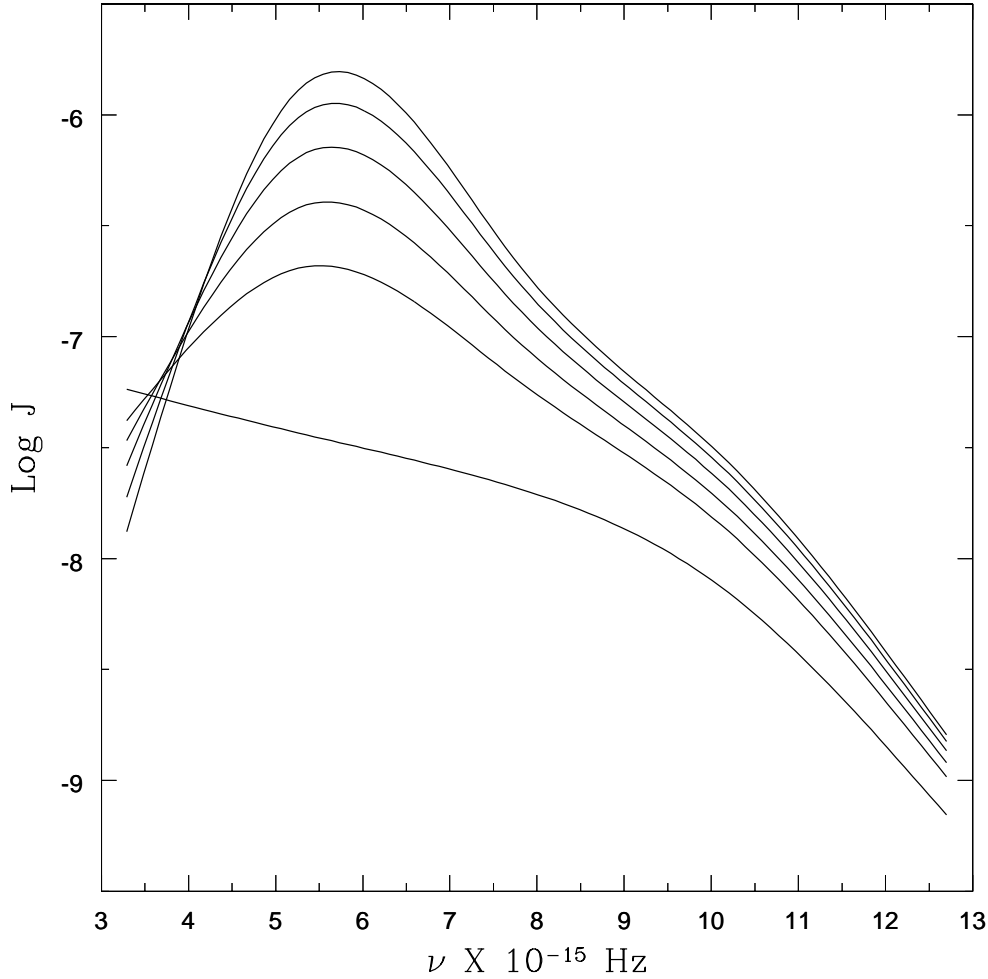


Fig. 2. Mean intensity without dust particles for different frequency points. From bottom to top the curves represent the models with terminal velocity  $V_t = 10, 20, 30, 50, 100$  and  $300 \text{ km s}^{-1}$  respectively.

with the increase in the velocity. The change in the mean intensity is maximum when the terminal velocity  $V_t$  is increased from  $10 \text{ km s}^{-1}$  to  $20 \text{ km s}^{-1}$ . Expansion of the medium yields the atmosphere diluted by decreasing the density. Hence more photons can escape from the bottom of the atmosphere. As a result, the mean intensity increases with the increase in velocity. For a dust-free atmosphere, the opacity is determined by the absorption cross section of Hydrogen and Helium. The absorption cross section for Hydrogen varies with the cube of the frequency while that for Helium changes exponentially. For small expansion velocity the mean intensity falls slowly with the increase in frequency up to  $10^{16} \text{ Hz}$  but then falls rapidly. This means the optical depth with small velocity is mainly governed by the change in the Hydrogen opacity. However, the Helium opacity starts dominating as the frequency increases from  $10^{16} \text{ Hz}$ . When the velocity increases, the mean intensity increases with

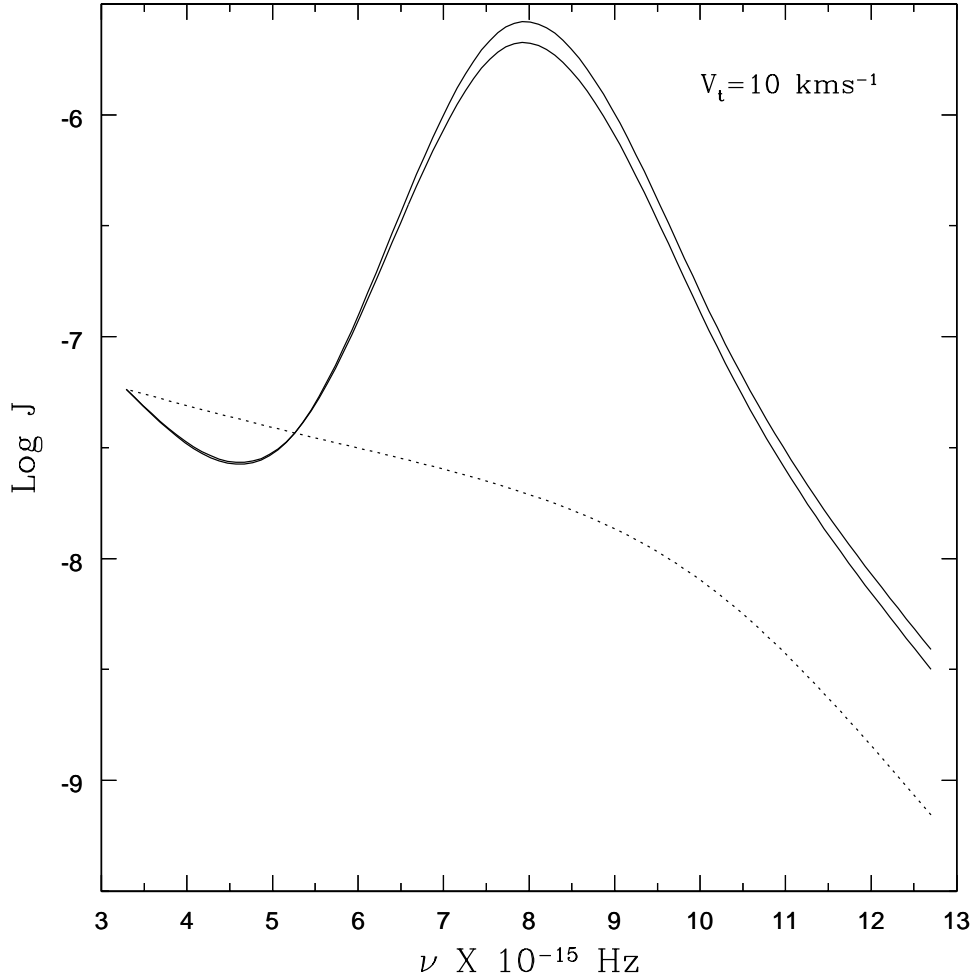


Fig. 3. Mean intensity with dust particles of different sizes and for  $V_t=10 \text{ km s}^{-1}$ . Top solid line represent the model with dust particles of radius  $0.5 \mu\text{m}$  while the bottom solid line represent the model with dust particles of radius  $0.1 \mu\text{m}$ . The dashed line represents the model without dust but with the same terminal velocity.

the increase in frequency and peaks at about  $5.5 \times 10^{15} \text{ Hz}$  and then falls rapidly. The change in the qualitative feature of the mean intensity with the increase in velocity is dictated by the change in the absorption cross-section while the increase in the intensity is due to the dilution of the medium.

With the incorporation of dust grains, there are significant qualitative as well as quantitative changes in the mean intensities as can be seen from figure 3 to figure 5. This is due to the fact that in a dusty atmosphere the optical depth is determined mainly by the dust. The absorption and scattering by dust are determined by the size and the refractive index of the grains. In the present investigation we have considered dust grain with sizes  $0.1 \mu\text{m}$  and  $0.5 \mu\text{m}$ . Given the high temperature of the medium, grains with larger

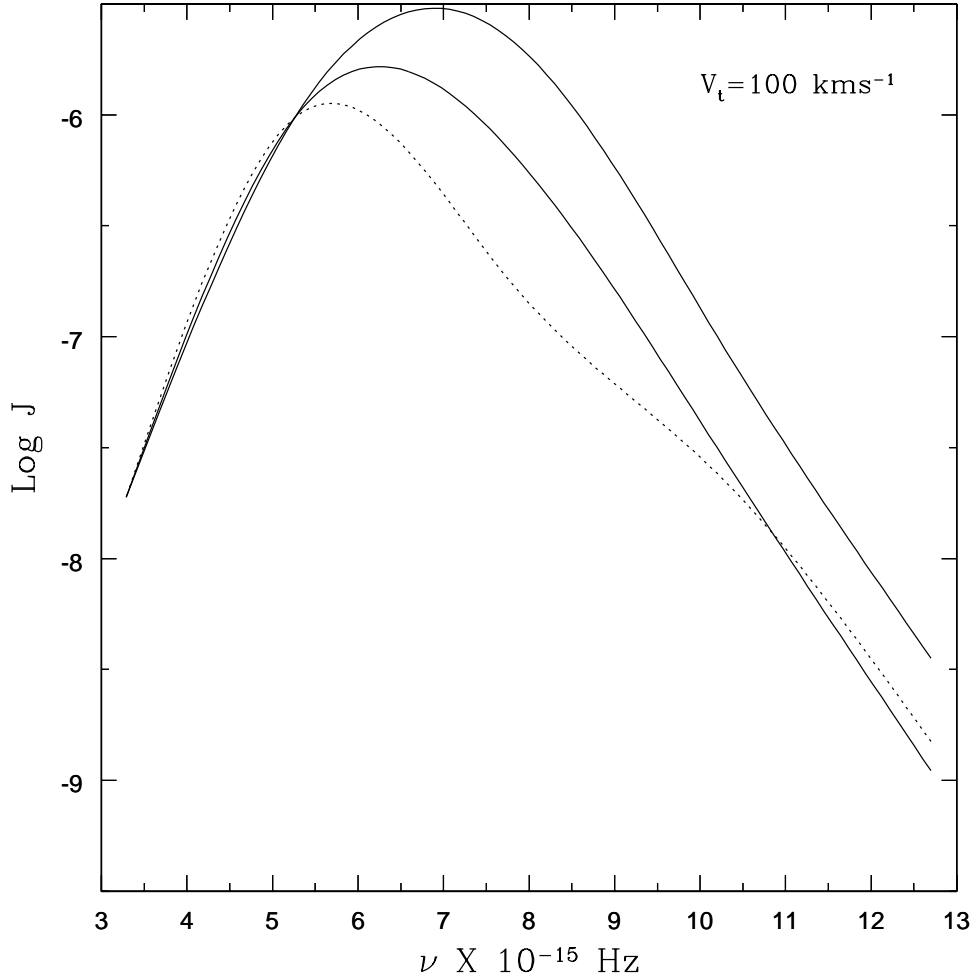


Fig. 4. Same as figure 3 but with  $V_t=100 \text{ km s}^{-1}$ .

size would not survive. Since the wavelengths under consideration is shorter than  $0.1 \mu m$ , scattering by dust plays a significant role in determining the mean intensity. It is well known that Rayleigh scattering is symmetric so that the amount of forward and backward scattering is the same. But, Mie scattering is asymmetric and it makes the forward scattering more than the backward scattering as discussed in section 4. This asymmetry increases as the ratio between the wavelength and the particle size increases. In a dust free clear atmosphere, a significant amount of radiation gets back scattered contributing to the reduction in mean intensity. But, dust scattering makes a large number of photons scattered in the forward direction yielding an increase in the mean intensity as compared to that without dust. With the adopted values for the wavelength and the particle size, dust scattering dominates over dust absorption. As a result, increase in mean intensity is obtained when dust is incorporated in the atmospheric models. The mean intensity increases with the increase in particle size as the asymmetry increases with the increase in

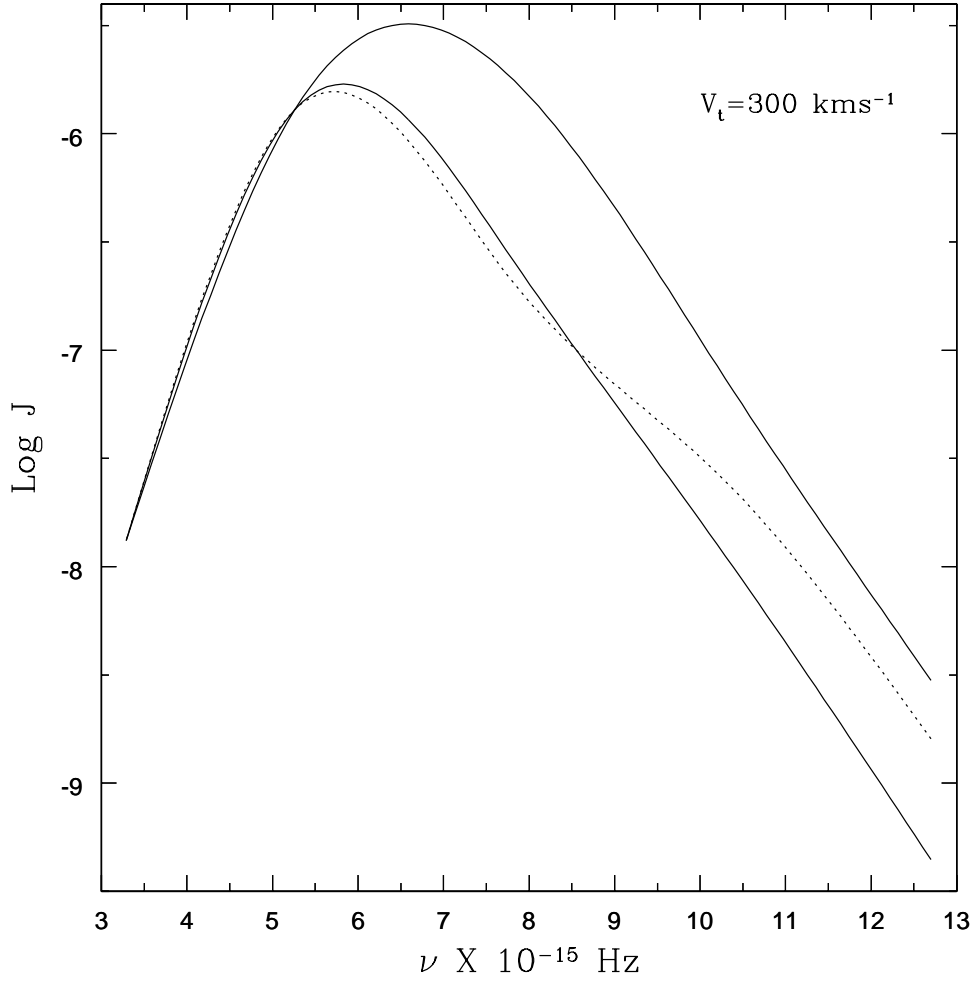


Fig. 5. Same as figure 3 but with  $V_t = 300 \text{ km s}^{-1}$ .

particle size. It is worth noting that the mean intensity for two different sizes of dust particles is the same for smaller frequency or longer wavelength and the changes in the mean intensity increases as one moves from smaller to larger frequencies.

## 7 Conclusion

The mean intensity from a planetary nebulae with expanding atmosphere is modeled by solving the radiative transfer equations for multiple scattering. Both dusty and dust-free medium is considered. For the dusty medium, Mie theory of scattering by spherical dust grains is employed. In a dust-free atmosphere, the mean intensity increases with the increase in the expansion velocity as the expansion of the medium removes matter causing a decrease in

optical depth. The entire intensity profile changes when dust scattering is incorporated. Due to the increase in forward scattering of photon by dust grains, the mean intensity increases significantly in a dusty medium as compared to that in a dust-free atmosphere. Also, the mean intensity increases with the increase in particle size. Thus it is shown that both the expansion and the presence of dust in the atmosphere of planetary nebulae play important role in determining the mean intensity of the object. The important implication of the present work is that even the presence of very small dust grain would affect the spectrum of planetary nebulae at the ultra-violet and near optical region. Therefore observation at shorter wavelengths would provide important information on the properties of dust grains as well as the velocity field.

## Acknowledgements

We are grateful to the anonymous referee for several useful suggestions and comments that has not only improved the quality of the manuscript substantially but also helped in removing some numerical errors.

## References

- [1] Amnuel, P. R., 1994, *Ap&SS*, 219, 117
- [2] Barlow, M. J., 1983, *Planetary Nebulae*, IAU Symp. No. 103, ed. Flower, D. R., p. 105, Reidel, Dordrecht, Holland
- [3] Bohren, C. F. & Huffman, D. R., 1983, *Absorption and Scattering of Light by Small Particles*, Wiley, New York
- [4] Chandrasekhar, S., 1960, *Radiative Transfer*, Dover, New York
- [5] Draine, B. T., and Lee, H. M., 1984, *ApJ*, 285, 89
- [6] Draine, B. T., 1985, *ApJS*, 57, 587
- [7] Harrington, J. P., 1968, *ApJ*, 152, 943
- [8] Harrington, J. P., 1969, *ApJ*, 156, 903
- [9] Hjellming, R. M., 1966, *ApJ*, 143, 420
- [10] Hoare, M. G., 1990, *MNRAS*, 244, 193
- [11] Hummer, D. J., and Seaton, M. J., 1963, *MNRAS*, 125, 437
- [12] Hummer, D. J., and Seaton, M. J., 1964, *MNRAS*, 127, 217
- [13] Iyengar, K. V. K., 1986, *A & A*, 158, 89



- [14] Kirk Patrick, R. C., 1970, ApJ, 162, 33
- [15] Kirk Patrick, R.C., 1972, ApJ, 176, 381
- [16] Koppen, J, 1979, 'A & AS, 35, 111
- [17] Koppen, J, 1980, A & AS, 39, 77
- [18] Landau, L. D., Lifshitz, E. M., 1975, The classical Theory of fields,4th Revised English Edition. Translated by Morton Hamermesh. Pergamon Press, Oxford. Page 117.
- [19] Osterbrock,D.E., 1974, Astrophysics of Gaseous Nebulae, Freeman, Sanfrancisco.
- [20] Peraiah, A., Grant, I. P., 1973, J. Inst. Math. Applc., 12, 75 (PG73)
- [21] Peraiah, A., Wehrse, R., 1978, A & A, 70, 213
- [22] Pottasch, S. R, Baud, B., Beintema, D., et al., 1984, A & A, 138, 10
- [23] Pottasch, S. R., 1987, In: Kwok, S., Pottasch, S. R. (eds.) Late Stages of Stellar Evolution, Reidel Publ. Co.
- [24] Ratag, M. A., Pottasch, S. R., Zijlstra, A. A., et al., 1990, A & A, 233, 181
- [25] Rubin, R. H., 1968, ApJ, 153, 761
- [26] Scott, A., & Duley, W. W., 1996, ApJS, 105, 401
- [27] Stasinska, G. & Szczerba, R., 1999, A & A, 352, 297
- [28] van de Hulst, H. C. 1957, Light Scattering by Small Particles, Wiley & Son, New York
- [29] Zijlstra, A., A., te Lintel Hekkert P., Pottasch, S. R., et al., 1989, A & A 217, 157

## A Appendix

The transmission and reflection operators as are given by,

$$\begin{aligned}
 t(n+1, n) &= t^+ [\Delta^+ S^{++} + r^{+-} r^{-+}] \\
 t(n, n+1) &= t^- [\Delta^- S^{--} + r^{-+} r^{+-}] \\
 r(n+1, n) &= 2t^- r^{-+} \Delta^+ M \\
 r(n, n+1) &= 2t^+ r^{+-} \Delta^- M
 \end{aligned} \tag{A.1}$$

and the source vectors are

$$\begin{aligned}
\Sigma^+ &= (1 - \omega_g)\tau_g t^+ [\Delta^+ B^+ + r^{+-} \Delta^- B^-] \\
\Sigma^- &= (1 - \omega_g)\tau_g t^- [\Delta^- B^- + r^{-+} \Delta^+ B^+]
\end{aligned} \tag{A.2}$$

where

$$\begin{aligned}
\Delta^+ &= [M + \frac{1}{2}\tau_g^+(I - Q^{++}) - \frac{1}{4}\tau_d P^{++} C]^{-1} \\
\Delta^- &= [M + \frac{1}{2}\tau_g^-(I - Q^{--}) - \frac{1}{4}\tau_d P^{--} C]^{-1}
\end{aligned} \tag{A.3}$$

$$\begin{aligned}
S^{++} &= M - \frac{1}{2}\tau_g^+(I - Q^{++}) + \frac{1}{4}\tau_d P^{++} C \\
S^{--} &= M - \frac{1}{2}\tau_g^-(I - Q^{--}) + \frac{1}{4}\tau_d P^{--} C
\end{aligned} \tag{A.4}$$

$$\begin{aligned}
S^{+-} &= \frac{1}{2}\tau_d Q^{+-} - \frac{1}{4}P^{+-} C \\
S^{-+} &= \frac{1}{2}\tau_d Q^{+-} - \frac{1}{4}P^{-+} C
\end{aligned} \tag{A.5}$$

$$\begin{aligned}
Q^{++} &= \frac{1}{2}\omega P^{++} C - \frac{\rho_c \Lambda^+}{\tau_g} \\
Q^{--} &= \frac{1}{2}\omega P^{--} C + \frac{\rho_c \Lambda^+}{\tau_g} \\
Q^{+-} &= \frac{1}{2}\omega P^{+-} C - \frac{\rho_c \Lambda^-}{\tau_g} \quad Q^{-+} = \frac{1}{2}\omega P^{-+} C + \frac{\rho_c \Lambda^-}{\tau_g}
\end{aligned} \tag{A.6}$$